

REDUNDANT ROTATING MEASUREMENTS IN AN AXIAL COLD FLOW TEST TURBINE – Development and Procedure

Fridh, J., Fransson, T.

Royal Institute of Technology (KTH)
Div. of Heat and Power Technology
SE-100 44 Stockholm
SWEDEN

Andersson, N-E., Magnusson, P.

Siemens Industrial Turbomachinery AB
SE-612 83 Finspong
SWEDEN

ABSTRACT

A rotating measurement system has been designed and commissioned for a cold flow test turbine and tested under the influence of partial admission. A shrouded turbine rotor of impulse design is equipped with miniature pressure transducers and strain gauges. This paper discusses the selected experimental design and procedure. Overall, the first test runs went well and necessary data were collected and could be evaluated accordingly. Encountered specific measurement technique problems are addressed where the importance of high redundancy is stressed. Results demonstrate one effect that imbedded sensor technology may encounter as regards of dynamic measurements and calibrations.

INTRODUCTION

In partial admission turbines, high circumferential pressure gradients exist that generate unsteady flows associated with pumping- and filling/emptying phenomena. And, from the mechanical point of view, the highly dynamic rotor loads act abusively on the downstream rotor blades and disc. The inherent dynamic flow nature in turbines under the influence of partial admission requires fast response sensors in order to satisfactorily capture the unsteady phenomena during experiments. For this purpose a rotor instrumented with miniature fast response measurement gauges has been taken into service in an axial air test turbine at the Royal Institute of Technology (KTH), Sweden, in collaboration with Siemens Industrial Turbomachinery AB.

NOMENCLATURE

a	speed of sound, m/s
f	frequency, Hz
j	complex variable, $j = \sqrt{-1}$
p	pressure, kPa
G	complex transfer function

g	gravitational acceleration, m/s^2
k	wave number, [1, 2, 3, ...]
L	tube length, m
ω	frequency, rad/s

Subscripts

ref	associated to reference sensor
$sens$	associated to sensor
$pitot$	associated to pitot tube opening

THE TEST OBJECT AND ACQUISITION

A 1 MW compressor with a maximum pressure of 4 bar(a) and a maximum mass flow of 4.7 kg/s, drives the cold flow (30-80°C) air test turbine in an open loop with a water brake to control the turbine power output. A detailed description of the test turbine and its diversified capabilities can be found in Fridh et al (2004).

The turbine is of subsonic impulse design and has endwall contouring at the stator casing. The rotor has two lacing wires rolled into the blades' shroud. The partial admission is achieved by introducing aerodynamically shaped filling blocks of various circumferential lengths, depending on admission degree, which occupy a partial volume in the annulus upstream the first stator row. Figure 1 shows the filling block and a cross section of the two-stage turbine where the first rotor is redundantly instrumented with piezoresistive miniature absolute pressure transducers and semi-conducting strain gauges.

The measuring signals from the rotating system are transferred, without any pre-amplification, via a miniature D-SUB (military standard) connector at the center of the rotor disc through high-speed brush slip rings (36 circuits) shown in Fig. 2. Here, a slip ring channel has typically an amplitude noise level less than 20 mΩ at 3600 rpm with an input voltage of 6 VDC and a current of 50mA, according to the delivery notes.

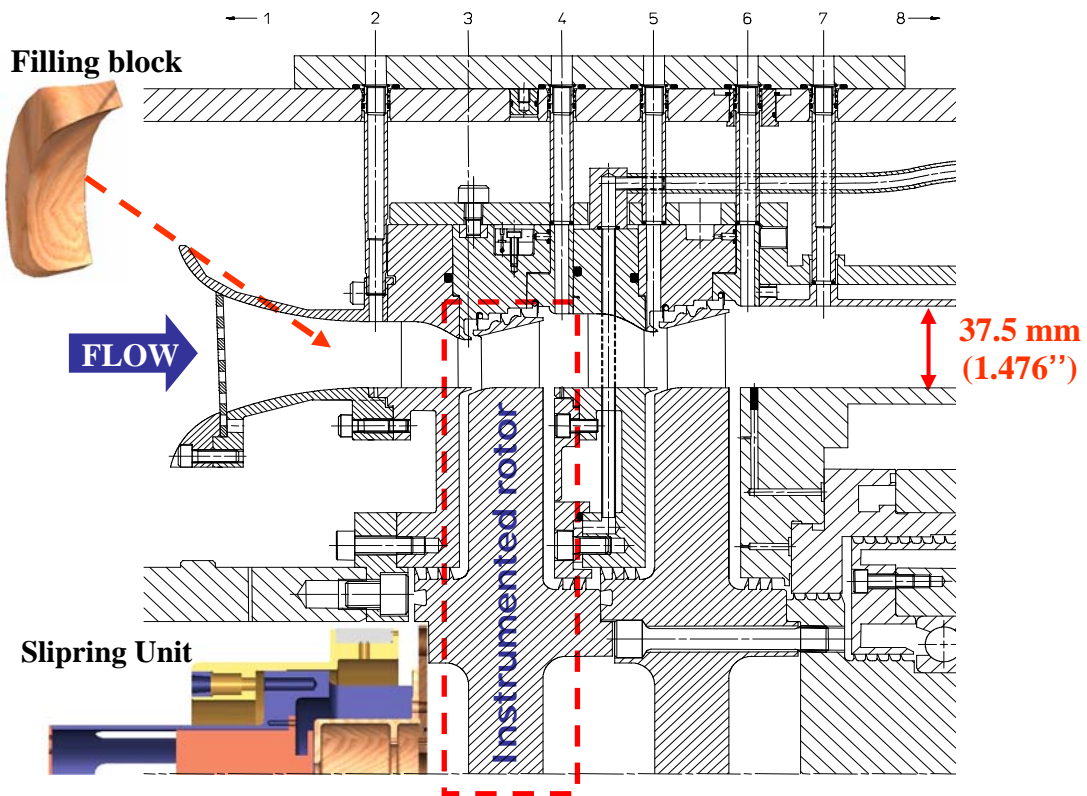


Figure 1: the test object

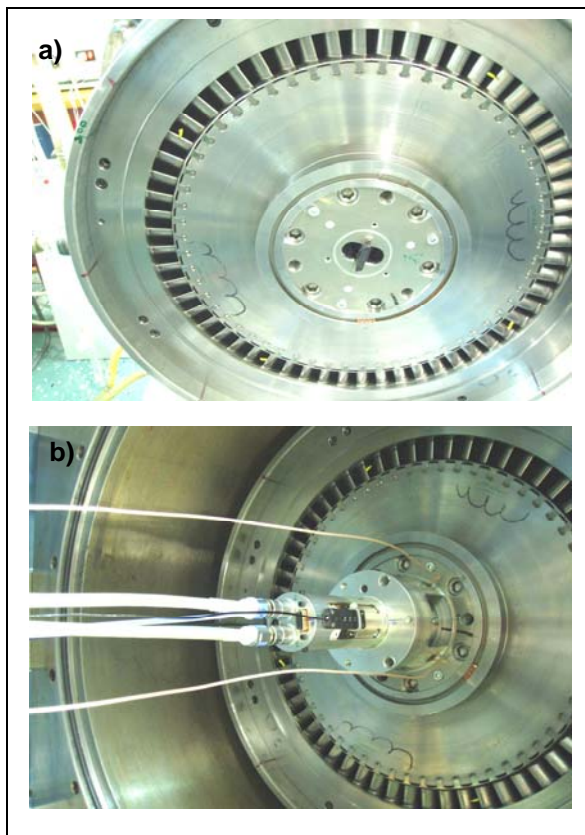


Figure 2: slipring system

- a) rotor disc with connector in center
- b) slipring unit mounted on rotor, during assembly

The signals are sampled at a frequency of 100 kHz per channel in a high-speed data acquisition system. The strain gauge signals are fed via a constant current AC-amplifier prior to the acquisition system. Optical sensors of reflective type, together with a tooth wheel were employed to retrieve once-per-revolution (OPR) and once-per-blade (OPB) reference pulses.

Two eddy current sensors were employed in order to monitor the rotor oscillations at the slip ring position. Furthermore, two thermo couples were used to monitor slip-ring temperatures.

The redundant instrumentation consists of four, individually excited, miniature pressure transducers mounted in four rotor blades with the purpose of measuring the total pressure in the relative frame of reference at midspan, rotor inlet. Diametrically opposed each other, two of the pressure sensors (Kulite XCQ-2-062) are mounted 0.4 mm recessed in pitot tubes that were aligned with the computed average relative flow angle. The pitot tubes have bevelled (60°) openings, which are positioned 1.5 mm axially upstream of the leading edge of the rotor blade as depicted in figure 3.

It is difficult to interpret relative total pressure measurements as clearly pointed out by Sieverding and Dénos (1992) due to the strong dependence of local static pressure. However, Dénos (2002) noted an improved agreement between relative total pressure measurements at the leading edge of a

rotor blade and static pressure measured at the stagnation point if a bevelled opening was used. In this study, also a distinct stagnation point is needed due to large variations in the flow angle, especially downstream of the sector ends of the admission jet.

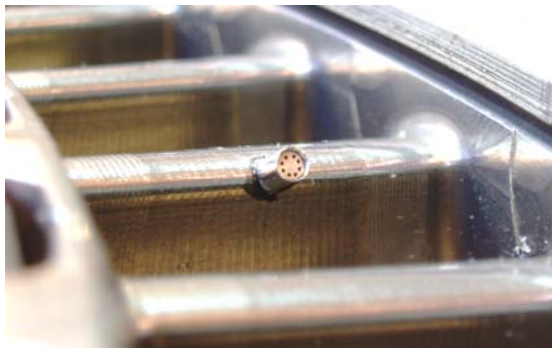


Figure 3: pressure transducer mounted in blade

The other two sensors (Kulite LQ-3-062) were mounted on cylindrical pins and put inside two rotor blades (diametrically opposed) and in contact with the flow channel through 10 mm long pitot tubes, also with bevelled openings.

The main reasons for using two different types of sensors were that they can withstand different acceleration and to be able to evaluate different sensor locations. The rated acceleration capabilities for sensor type XCQ-2-062 is 10'000g and for the other sensor type 30'000g. Although the design operating point implies g-load of 4'200g at sensor location, other operating points in the measurement campaign yield g-loads in the vicinity of 10'000g.

When employing piezoresistive pressure transducers for unsteady measurements, particularly in rotating systems, five main considerations should be addressed; temperature effects, fundamental accuracy, base strain sensitivity, acceleration sensitivity and the frequency response. These are exemplarily and methodically investigated by Ainsworth et al (2000). Here, the pressure transducers are equipped with temperature compensating modules. Static and dynamic pressure calibrations pre- and post tests are performed to limit the errors. Also, the calibrations were performed, in-situ with the slipping system connected. The base strain influence is estimated to be negligible due to the use of commercial transducers with strain isolating pedestal and the mounting in a pitot tube or on a pin also probably reduces the strain at the transducer location. Furthermore, the rotor disc has, prior to the instrumentation, been balanced at 10'000 rpm, which has set the bladed disc system in order to avoid unexpected movements. All pressure sensors were positioned such that the transducer membrane was transverse to the centrifugal load. In order to account for the inertia effects of the transducer, a software correction for

the acceleration was performed in the post processing according to typical acceleration sensitivity ($4 \cdot 10^{-5}$ % of F.S. /g) reported by Kurtz et al (2000). The frequency response of the cylindrical sensors is somewhat lowered due to the mounting but is estimated to be sufficient for the maximum wake passing frequency of 3.1 kHz, and dynamic calibrations up to 3.6 kHz reveals very small influences in magnitude and phase. However, the frequency response is significantly reduced for the two imbedded sensors, which turned out to be difficult calibrating dynamically (discussed later).

Furthermore, eight semi-conducting strain gages are mounted at various positions where the computed strains are high on the rotor blades in order to detect dynamic strains. Four blades have a gauge mounted on the shroud surface exposed to the flow, in the tangential direction and same axial position as the downstream lacing wire. Four blades have gauges on the downstream surface of the rotor bulb neck where two are sensing tensile and two compressive strains, primarily. Figure 4 gives an illustrative picture on where the gauges are located.

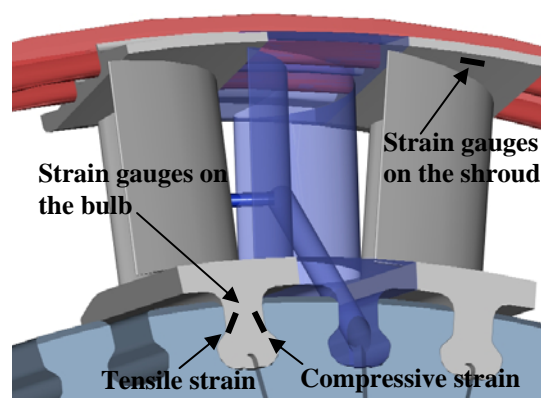


Figure 4: illustrated sensor locations (downstream view)

One should be aware of the non-linear temperature sensitivity of semi-conducting strain gauges, which is described for example by Figliola and Beasley (2000), and can if desired, be compensated either hardware-wise by compensating resistors or by software corrections based on calibration curves. However, here semi-conducting gauges with a high gage factor (130.5) is strived for, partly because no signal amplification exists in the rotating system and partly the relatively small aerodynamic blade loads to be detected. Furthermore, the temperature variations are moderate and no absolute force levels are sought in these trials rather the relative variations. The cylindrical gauge (BLH SP5-06-35, 350 Ω) is 2mm long with a diameter of 0.2mm.

All the instrumentation has been done pairwise, diametrically opposed in order to reduce any

unnecessary unbalance, and balancing tests performed post instrumentation revealed that no correction was necessary.

Measurement System Setup

The operating point is achieved by changing the rotational speed by controlling the brake power while the static pressure ratio is kept constant for the turbine, which is supervised via the steady measurement system (not described further here) that acquires and logs the requested time-averaged data. The synchronous fast measurement system acquires the signals from the rotating system and once-per-revolution (OPR) and once-per-blade (OPB) pulses from the optical reflective switches (maximum switching frequency of 50 kHz) detected from a tooth wheel. An OPR reference mark (rotor-zero) on the rotor is aligned with the absolute machine zero position with the help of a laser before the measurements.

The strain gauge signals are individually amplified using FYLDE dynamic (AC, balanced DC) strain gauge amplifiers with constant current supply, which have a frequency response of up to 50 kHz and here a gain in the order of 150 is used to reach a 100 mV/ μ Strain output.

The unsteady measurement signals are acquired by means of a digital high-speed data acquisition system (Kayser Threde KT8000), which also provides stabilized 10VDC excitation for the pressure transducers. The system has a 14 bit A/D conversion for each channel. The analogue pressure signals are amplified with a gain of 50 without filtering and sampled at a rate of 100 kHz.

Data evaluation and dynamic calibration

In the post processing, firstly, static calibration coefficients are applied for the pressure signals. Secondly the acceleration effects are accounted for before applying transform characteristics from the dynamic calibrations. Ensemble average values for one rotational cycle are calculated out of typically 300 rotations (at 4450rpm) with the help of the OPR and OPB pulses.

The propagation of pressure transients in tubes and cavities attenuates the true pressure signal and give rise to a phase lag. Even for short tubes and small cavities this may be of importance. Therefore, a dynamic transfer function is applied to the signal. The calibration procedure is performed in accordance with Vogt and Fransson (2004). A reference pressure pulse signal generated by a rotating hole-disc system described by Vogt (2001), is applied to a miniature cavity (containing a flush mounted reference sensor) placed on the instrumented blade. For each measured frequency, the dynamic transfer characteristics have been determined from the harmonic components of the sensor and reference signals, according to Eq. (1).

$$G(j\omega) = \frac{\hat{p}_{sens}(j\omega)}{\hat{p}_{ref}(j\omega)} \quad (1)$$

The dynamic transfer characteristics were determined only for frequencies up to 4 kHz, which here is the maximum frequency of the pressure pulse generator. Signals above 4 kHz were set to zero, which effectively means that the dynamic calibration will work as a low-pass filter. In accordance with Vogt and Fransson (2004), the signal at the pitot tube opening can be obtained from signal reconstruction in the frequency domain by applying the inverse dynamic transfer function to the sensor signal according to Eq. (2).

$$\hat{p}_{pitot}(j\omega) = G^{-1}(j\omega) \cdot \hat{p}_{sens}(j\omega) \quad (2)$$

RESULTS AND DISCUSSION

Commissioning ran smoothly and data with low noise to signal ratios have been recorded at desired operating points with rotational speeds up to 4500 rpm.

Early on during the tests, three of the strain gauges showed erratic signals that could not be derived to any flow or machine related phenomena. This is believed to be due to bad gauge attachment on the surface since the gauge resistances were still in the right range which indicates unbroken wirings.

Due to low aerodynamic forces and mounting on a pre-existing rigid rotor disc with coupled blades at the shroud (lacing wires), the strain gauge signals were of low amplitudes. A moving average with a window size of 64, which corresponds to approximately two stator pitches, was used in order to observe trends. It is worth noting the impact a moving average will have on signal transients. Figure 5 shows the post processed data from one strain gauge positioned on the shroud, and where the window size is varied.

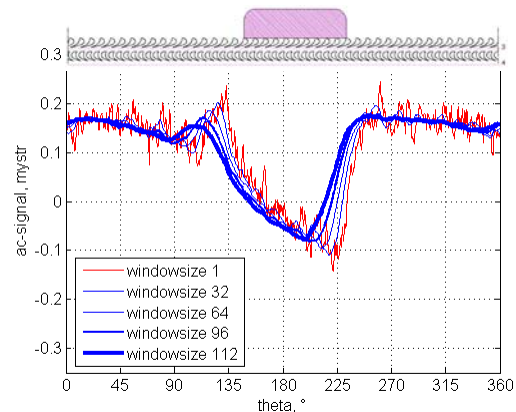


**Figure 5: moving average effects
(ensemble average data, ~300 rotations)**

The dynamic strain value (μ Strain) is plotted versus the circumferential position of the gauge, in relation to the depicted stage (with the indicated partial admission blockage). Not surprisingly, it is seen that the peak and dip at the admission sector gradients are shifted circumferentially with an increased window size. In this case the moving average has been evaluated from 0 to 360 degrees.

Figure 6 shows the normalized pressure signals (ensemble averaged) from the four employed pressure sensors before applying dynamic transfer

characteristics. B18 and B47 represent the imbedded sensors. It is clearly seen in Fig. 6 that the pressure signals from B18 and B47 are not at all following the trends of the other (B03 and B32) sensors, which are mounted close to the pitot opening. Ideally, this should be corrected when applying dynamic transfer characteristics resulting in the lines collapsing on each other.

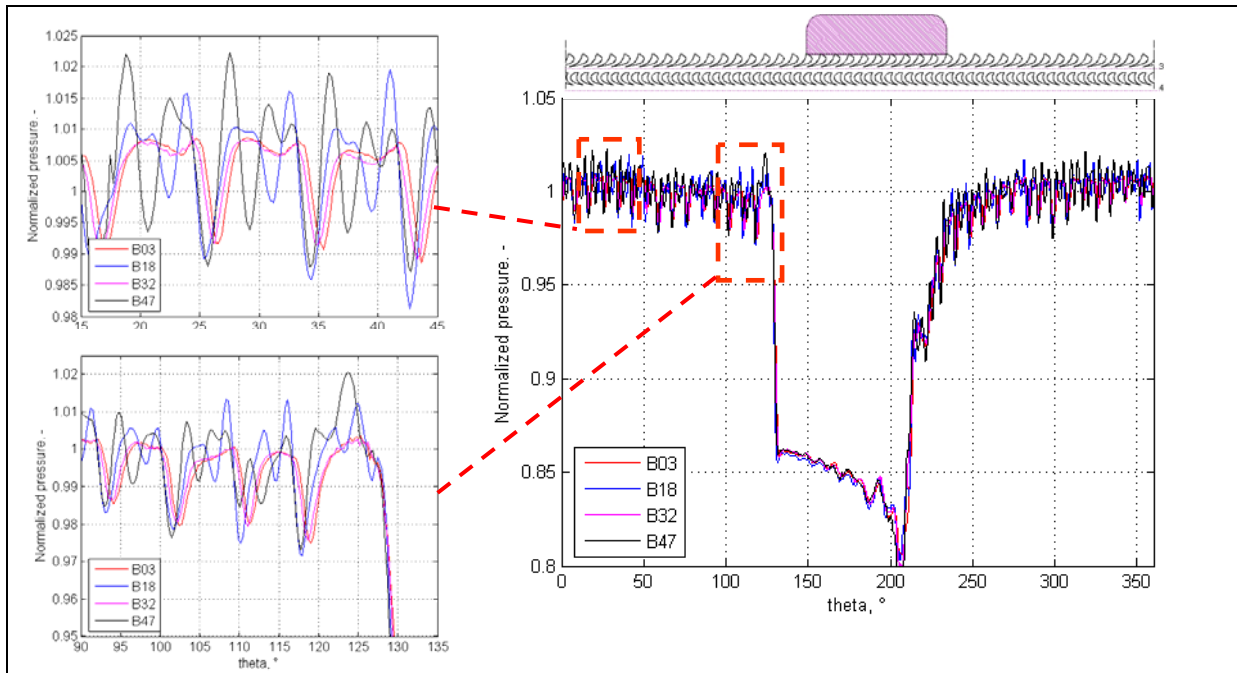


Figure 6: normalized pressure signals for blade sensors, before applying dynamic transfer function

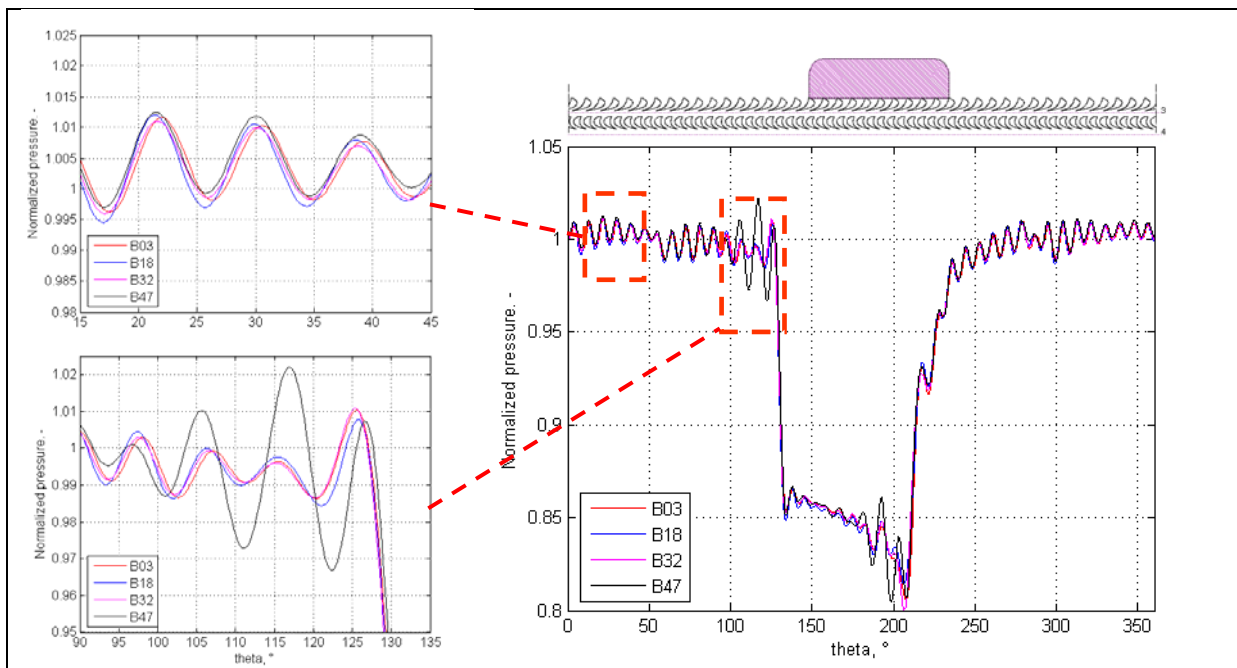


Figure 7: normalized pressure signals for blade sensors, after applying dynamic transfer function

However, this is not the case for one of the imbedded sensors (B47), in vicinities of the admission jet. Figure 7 shows the dynamically calibrated data where it is duly noted that the amplitude and phase of sensor B47 is not in line with the other sensors at the sector ends.

According to Fridh et al (2004) there is a prompt redirection of the flow downstream of the sector ends due to high circumferential static pressure gradients, which locally decreases the stator wake frequency. And, by viewing the transfer properties in Fig. 8 (from dynamic calibrations) a resonance frequency is observed for the B47 sensor, which is in the range of the local stator wake frequency at sector ends (1.5-2 kHz) that seems to excite this resonance frequency. The stator wake frequency at full admission is 3.1 kHz at the design speed.

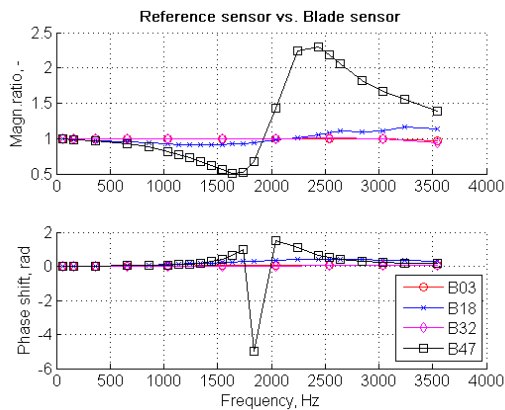


Figure 8: dynamic transfer properties for pressure sensors

Even though detailed dynamic calibrations are attempted, the pressure signal cannot, here, be completely reconstructed close to sector ends. The anticipated frequency response for the imbedded sensor was in the range of 10 kHz based on calculation of the first harmonic organ pipe frequency in the pitot tube.

The organ pipe approach implies that a $\lambda/4$ wave will establish in the pitot tube or any present capillarity cavity that yields the resonance frequencies according to Eq. (3).

$$f = k \cdot \frac{a}{4L}, \quad k = 1, 2, 3, \dots \quad (3)$$

One suggested explanation of the resonance frequency in Fig. 8 is that a cavity, in which an organ pipe resonance can occur, exists along the cylindrical pin onto which the sensor is mounted. The length of the pin corresponds quite well with the arisen resonance appearing in the dynamic calibration. Figure 9 shows a sketch of the blade

with the imbedded sensor. Problem analysis has shown that the mechanical mounting for the imbedded sensor is complex and sensitive for imperfections. The principal mounting procedure is as follows: the sensor is mounted at its location on the cylindrical pin then inserted in the prepared blade, and then the pitot tube is mounted and sealed, and finally fixing and sealing of the cylindrical pin as indicated in Fig. 9. This procedure, perhaps together with the centrifugal force, is suspected to cause a leakage at the inner parts of the pitot tube, which facilitate air flow along the side of the cylindrical pin.

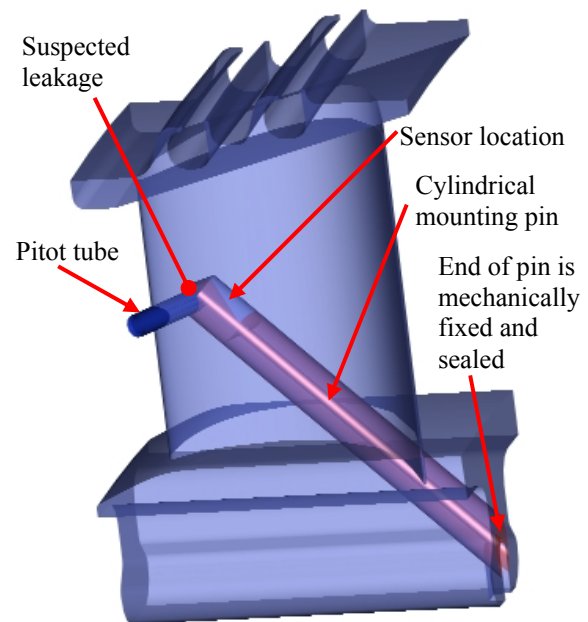


Figure 9: rotor blade with imbedded sensor

CONCLUDING REMARKS

A rotating measurement system has been presented and discussed with focus on the measurement techniques used. Concluding remarks are bulleted below.

- The commissioning of the system was successful and data with low noise to signal ratios have been recorded at desired operating points in a partial admission turbine with rotational speeds up to 4500 rpm.
- Three failing strain gauges have been reported.
- One pressure sensor showing ‘untrustworthy’ signal due to suspected internal leakage leading to an ‘organ pipe’ resonance excited by a local decrease in the stator wake frequency adjacent to sector ends.
- Because of a deliberately chosen high redundancy of the instrumentation, the failing and untrustworthy gauges do not affect the

evaluation of studied parameters appreciably. Nevertheless, the overall outcome demonstrates the importance to establish a redundant system when performing rotating measurements, which can contain many “unknowns”.

Vogt, D. and Fransson, T. (2004), *A Technique for Using Recessed-Mounted Pressure Transducers to Measure Unsteady Pressure*, Proc. of the 17th Symp. on Measuring Techniques for Transonic and Supersonic Flow in Cascade and Turbomachines, Stockholm, Sep. 2004

ACKNOWLEDGMENTS

The Swedish National Energy Administration (contract 12457) and Siemens Industrial Turbomachinery AB, Finspong, are gratefully acknowledged for the financial support related to this work. Furthermore, we would like to direct our special thanks to all our colleagues at KTH and Siemens for all the valuable help, and especially Rolf Bornhed, Leif Ruud, Lars Malmlov and Sven-Gunnar Sundqvist.

REFERENCES

- Ainsworth, R.W., Miller, R.J., Moss, R.W., Thorpe, S.J. (2000), *Unsteady Pressure Measurements*, Meas. Sci. Technol. **11** (2000), pp.1055-1076
- Dénos, R. (2002), *Influence of Temperature Transients and Centrifugal Force on Fast-response Transducers*, Experiments in Fluids **33** (2002), pp. 256-264
- Figliola, R. and Beasley, D. (2000), *Theory and Design for Mechanical Measurements*, 3rd Ed., John Wiley & Sons, Inc., 2000, ISBN 0-471-35083-4
- Fridh, J., Bunkute, B., Fakhrai, R., Fransson, T. (2004), *An Experimental Study on Partial Admission in a Two-Stage Axial Air Test Turbine with Numerical Comparisons*, Proc. of ASME Turbo Expo 2004 conf., paper No. GT 2004-53774
- Kurtz, A.D., Ainsworth, R.W., Thorpe, S.J., Ned, A. (2000), *Acceleration Insensitive Semiconductor Pressure Sensors for High Bandwidth Measurements on Rotating Turbine Blades*, Proc. of the 15th Symp. on Measuring Techniques for Transonic and Supersonic Flow in Cascade and Turbomachines, Florence, Sep. 2000
- Sieverding, C.H. and Dénos, R. (1992), *Relative Total Pressure Measurements Downstream of a Transonic Annular Cascade*, Proc. of the 11th Symp. on Measuring Techniques for Transonic and Supersonic Flow in Cascade and Turbomachines, Munich, Sep. 1992
- Vogt, D. (2001), *A New Pressure Pulse Generator for Dynamic Calibration*, HPT internal report KTH/HPT-01-10, Stockholm, 2001